Eur. Phys. J. D **29**, 95–103 (2004)
DOI: 10.1140/epjd/e2004-00018-2

THE EUROPEAN PHYSICAL JOURNAL D

On the bichromatic excitation of a two-level atom with squeezed light

Amitabh Joshi[a], Reeta Vyas, Surendra Singh, and Min Xiao

Department of Physics, University of Arkansas, Fayetteville AR 72701, USA

Received 3 September 2003 / Received in final form 11 November 2003
Published online 17 February 2004 –

Abstract. Analytical results for the dynamical evolution of a single two-level atom coupled to an ordinary heat bath and bichromatically excited with two finite bandwidth squeezed fields are presented by solving the Heisenberg equations of motion. Photon statistics of the system in terms of the second-order intensity-intensity correlation function are also discussed. Transient fluorescent intensity as well as intensity correlation function exhibit oscillatory phenomenon even in the weak field limit. The latter also shows enhanced delayed bunching effect. All these effects are sensitive to the bandwidth of squeezed light.

PACS. 42.50.Ct Quantum description of interaction of light and matter; related experiments – 42.50.Dv Nonclassical states of the electromagnetic field, including entangled photon states; quantum state engineering and measurements

1 Introduction

Studies related to the dynamical evolution, the photon statistics, spectral and radiative properties of one and many two-level atoms embedded in a broadband squeezed bath have been the topics of keen interest in quantum optics. Gardiner [1] studied the interaction of a two-level atom with a broadband squeezed bath and predicted unequal polarization quadrature-decay rates. Carmichael, Lane and Walls [2] were able to discover a significant phenomenon of sub-natural linewidth in the fluorescence spectrum of a driven two-level atom, in the presence of squeezed light. Atomic absorption spectrum was discussed by Ritsch and Zoller [3] in the presence of colored squeezed vacuum. Since then many interesting results in atom-squeezed field interaction have been reported which include both two and three-level atoms interacting with broad bandwidth or narrow bandwidth squeezed baths [4, 5]. In a recent study the interaction of a two-level atom with the squeezed vacuum of bandwidth smaller than the natural atomic linewidth was considered and the hole burning and the three-peaked structure in spectra of fluorescence and transmitted field were predicted [6]. These results essentially show that squeezed fields having pairwise correlations and anisotropic noise distribution can give rise to interesting phenomena including novel features in spectral properties of atoms, formation of pure states and photon statistics. A more realistic model of finite bandwidth squeezed light interacting with a single two-level atom has been studied by Vyas and Singh [7] and Lyublinskaya and Vyas [8] where the source of the squeezed light employed was a degenerated parametric oscillator (DPO) operating below threshold and a homodyned DPO [9]. In another work, a two-level atom inside an optical parametric oscillator has been considered and hole and dips in the fluorescence and transmitted light has been observed [10]. The interest in other sources of squeezed light as well as its applications in a wide variety of areas has continued unabated [11–13].

The interaction of a single two-level atom with bichromatic driving field has also been studied extensively both theoretically and experimentally [14]. These studies were motivated by the observations that the bichromatic nature of the driving field can lead to a number of novel features which are different from the monochromatic case. For example, the fluorescence intensity exhibits resonances at subharmonics of the Rabi frequency and different spectral characteristics when compared with the usual Mollow triplet. Recently, some new calculations for resonance fluorescence and absorption spectra of a two-level atom driven by bichromatic field have been reported [15]. Also, reported are the effects of broadband squeezed reservoir on the second order intensity correlation function and squeezing in the resonance fluorescence for a bichromatically driven two-level atom [16]. Coherent population trapping and Sisyphus cooling under bichromatic illumination have also been studied [17]. In another recent work the electromagnetically induced transparency (which normally occurs in three-level atoms) has been demonstrated in a two-level atom excited by a bichromatic field (one strong and one weak field) and possibility of squeezed-light generation has also been discussed [18].

In this work, we study the interaction of a single two-level atom with a bichromatic electromagnetic field that is

[a] e-mail: ajoshi@uark.edu

produced from two independent DPOs. Unlike the broadband squeezed bichromatic excitation considered in earlier studies, the DPO produces finite bandwidth squeezed light. Furthermore, the earlier investigations were confined to the study of spectral changes that arise in broadband squeezed fields. The motivation behind our study is to investigate new features in the dynamical evolution and photon statistics arising due to bichromatic excitation of atom by finite bandwidth squeezed fields. It is useful to recall that unlike a coherent source, squeezed light is characterized by highly bunched photon sequence displaying strong pairwise correlations. This difference in the underlying photon statistics is clearly reflected in the fluorescent light from the atom under bichromatic illumination. We will see in the following that in the time evolution of both transient fluorescent intensity as well as the second order intensity correlation function there are oscillations present due to the bichromatic excitation. We also observe enhanced delayed bunching effect in this system. Both of these are sensitive to the bandwidth of squeezed light. Under coherent field excitation such effects are observed at much higher intensities.

The model of squeezed light adopted here corresponds to light from a degenerate parametric oscillator operating below threshold. This field can be modelled by two real Gaussian processes with different variances and correlation times [9]. Because of the finite correlation time of incident field, atomic states and the field states develop correlations during their dynamical evolution leading to novel features in the photon statistics of the fluorescent field.

The organization of the paper is as follows: in Section 2 we present the model and derive the equations of motion governing the time evolution of atomic and field operators. Solutions of these equations are used to discuss the time-evolution of fluorescent light intensity in Section 3. We discuss field statistical properties in terms of the second-order intensity-intensity correlation function in Section 4. In Section 5 we summarize the results of this paper and give some concluding remarks.

2 The model and equations of motion

We consider a two-level atom with energy level separation $\hbar\omega_0$, and allow it to interact with bichromatic field of frequencies $\hbar(\omega_0 \pm \delta)$. The atom is stationary and located at origin ($r = 0$). The Hamiltonian for such a system in the dipole (i.e., atom is localized well within the wavelength of light) and rotating wave approximation (RWA) is

$$\hat{H} = \hbar\omega_0\hat{S}_z + i\omega_0\wp\left[\hat{\mathcal{A}}_1^-(0,t)\hat{S}_-(t) - \hat{\mathcal{A}}_1^+(0,t)\hat{S}_+(t)\right] + i\omega_0\wp\left[\hat{\mathcal{A}}_2^-(0,t)\hat{S}_-(t) - \hat{\mathcal{A}}_2^+(0,t)\hat{S}_+(t)\right] + \hat{H}_{field}. \tag{1}$$

Here, $\hat{S}_\pm$, $\hat{S}_z$ are atomic operators for the two-level atom satisfying the following commutation relations:

$$\left[\hat{S}_+, \hat{S}_-\right] = \pm 2\hat{S}_z, \qquad \left[\hat{S}_z, \hat{S}_\pm\right] = \pm\hat{S}_\pm, \tag{2}$$

and $\hat{H}_{field}$ represents the energy of the electromagnetic field, $\wp$ is the transition dipole moment of the atom and $\hat{\vec{\mathcal{A}}}(0,t)$ is the vector potential at the position ($r = 0$) of the atom. We work in the standard Coulomb gauge so all the field vectors are transverse. The positive and negative frequency parts of the vector potential $\hat{\vec{\mathcal{A}}}_i(r,t)$ are represented by $\hat{\vec{\mathcal{A}}}_i^+(r,t)$ and $\hat{\vec{\mathcal{A}}}_i^-(r,t)$ (where $i = 1, 2$; as we have a bichromatic field), respectively. The two modes of the bichromatic field are symmetrically located on the two sides of the central frequency ω_0. We denote them by $\omega_1 = \omega_0 + \delta$ and $\omega_2 = \omega_0 - \delta$. Note that the atom considered here is a two state quantum system — a standard model in the quantum optics literature. If one considers two magnetic sub-levels then polarization state of light field is also to be specified.

The solutions of the Heisenberg equations of motion for the vector potentials $\hat{\vec{\mathcal{A}}}^\pm(0,t)$ contain a source term and a free field term as given by

$$\begin{aligned}\vec{\wp}\cdot\hat{\vec{\mathcal{A}}}^+(0,t) &= \frac{\hbar}{\omega_0}(\beta - i\Gamma)\hat{S}_-(t) + \vec{\wp}\cdot\hat{\vec{\mathcal{A}}}^+{}_{free}(0,t),\\ \vec{\wp}\cdot\hat{\vec{\mathcal{A}}}^-(0,t) &= \frac{\hbar}{\omega_0}(\beta + i\Gamma)\hat{S}_+(t) + \vec{\wp}\cdot\hat{\vec{\mathcal{A}}}^-{}_{free}(0,t),\end{aligned} \tag{3}$$

where $\hat{\vec{\mathcal{A}}}^\pm{}_{free} = \hat{\vec{\mathcal{A}}}_{1\,free}^\pm + \hat{\vec{\mathcal{A}}}_{2\,free}^\pm$ represent the solution of the homogeneous (source free) wave equation. The parameter β given by

$$\beta = \left(\frac{1}{4\pi\epsilon_0}\right)\frac{2}{3}\frac{\wp^2\omega_0^3}{\hbar c^3}, \tag{4}$$

is half of the Einstein A coefficient and Γ is the radiative frequency shift.

We can calculate the electric and magnetic fields corresponding to the vector potentials given in equation (3) [19]:

$$\begin{aligned}\hat{\vec{E}}^+(\hat{\vec{r}},t) &= \left(\frac{\omega_0^2}{4\pi\epsilon_0 c^2}\right)\frac{\hat{\vec{r}}\times(\hat{\vec{\wp}}\times\hat{\vec{r}})}{r^3} \times\hat{S}_-\left(t-\frac{r}{c}\right) + \hat{\vec{\mathcal{E}}}^+{}_{free}(r,t),\\ \hat{\vec{B}}^+(\hat{\vec{r}},t) &= \left(\frac{\omega_0^2}{4\pi\epsilon_0 c^2}\right)\frac{\hat{\vec{r}}\times\hat{\vec{\wp}}}{r^3 c}\hat{S}_-\left(t-\frac{r}{c}\right) + \hat{\vec{\mathcal{B}}}^+{}_{free}(r,t).\end{aligned} \tag{5}$$

These equations express the field variables in terms of the atomic variables. The first term is analogous to the radiation field of a classical oscillating dipole of strength $\wp S_-(t - r/c)$ at the origin and $\hat{\vec{\mathcal{E}}}^+{}_{free}(r,t)$ and $\hat{\vec{\mathcal{B}}}^+{}_{free}(r,t)$ are the free fields.

With the help of equation (1) we can write down the Heisenberg equations of motion for the atomic

operators as

$$\dot{\hat{S}}_-(t) = -i\omega_0\hat{S}_-(t) + \frac{2\omega_0}{\hbar}\hat{S}_z(t)\vec{\wp}\cdot\hat{\vec{\mathcal{A}}}_1^+(0,t) + \frac{2\omega_0}{\hbar}\hat{S}_z(t)\vec{\wp}\cdot\hat{\vec{\mathcal{A}}}_2^+(0,t),$$

$$\dot{\hat{S}}_z(t) = -\frac{\omega_0}{\hbar}\left(\hat{S}_-(t)\vec{\wp}\cdot\hat{\vec{\mathcal{A}}}_1^-(0,t) + \vec{\wp}\cdot\hat{\vec{\mathcal{A}}}_1^+(0,t)\hat{S}_+(t)\right) - \frac{\omega_0}{\hbar}\left(\hat{S}_-(t)\vec{\wp}\cdot\hat{\vec{\mathcal{A}}}_2^-(0,t) + \vec{\wp}\cdot\hat{\vec{\mathcal{A}}}_2^+(0,t)\hat{S}_+(t)\right). \quad (6)$$

The response of the atomic variables will be predominantly at frequency ω_0 and those of the field variables at frequencies ω_i $(i = 1, 2)$, respectively. We can then define slowly varying dynamical variables as

$$\hat{q}(t) = e^{i\omega_0 t}\hat{S}_-(t),$$
$$\hat{\vec{A}}^+_{i,\,free}(r,t) = e^{i\omega_i t}\hat{\vec{\mathcal{A}}}^+_{i,\,free}(r,t),$$
$$\hat{q}^\dagger(t) = e^{-i\omega_0 t}\hat{S}_+(t),$$
$$\hat{\vec{A}}^-_{i,\,free}(r,t) = e^{-i\omega_i t}\hat{\vec{\mathcal{A}}}^-_{i,\,free}(r,t), \qquad (i = 1, 2). \quad (7)$$

By substituting equation (7) in equation (6) we obtain

$$\dot{\hat{q}}(t) = -\beta\hat{q}(t) + \frac{2\omega_0}{\hbar}e^{-i\delta t}\vec{\wp}\cdot\hat{\vec{A}}^+_{1,free}(0,t)\hat{S}_z + \frac{2\omega_0}{\hbar}e^{i\delta t}\vec{\wp}\cdot\hat{\vec{A}}^+_{2,free}(0,t)\hat{S}_z, \quad (8)$$

$$\dot{\hat{S}}_z(t) = -2\beta\left[\hat{S}_z(t) + 1/2\right] - \left(\frac{\omega_0}{\hbar}\right)\left[e^{i\delta t}\vec{\wp}\cdot\hat{\vec{A}}^-_{1,free}(0,t)\hat{q}(t) + e^{-i\delta t}\vec{\wp}\cdot\hat{\vec{A}}^+_{1,free}(0,t)\hat{q}^\dagger(t)\right] - \left(\frac{\omega_0}{\hbar}\right)\left[e^{-i\delta t}\vec{\wp}\cdot\hat{\vec{A}}^-_{2,free}(0,t)\hat{q}(t) + e^{i\delta t}\vec{\wp}\cdot\hat{\vec{A}}^+_{2,free}(0,t)\hat{q}^\dagger(t)\right], \quad (9)$$

where 2δ is the separation between the two excitation mode frequencies. On integrating these equations formally, the slowly varying atomic operators $\hat{q}(t)$ and $\hat{S}_z(t)$ can be written as

$$\hat{q}(t) = e^{-\beta t}\hat{q}(0) + \frac{2\omega_0}{\hbar}\wp e^{-\beta t}\int_0^t dt_1 e^{(\beta-i\delta)t_1}\hat{A}_1(t_1)\hat{S}_z(t_1) + \frac{2\omega_0}{\hbar}\wp e^{-\beta t}\int_0^t dt_1 e^{(\beta+i\delta)t_1}\hat{A}_2(t_1)\hat{S}_z(t_1), \quad (10)$$

$$\hat{S}_z(t) + 1/2 = e^{-2\beta t}\left[\hat{S}_z(0) + 1/2\right] - \frac{2\omega_0}{\hbar}\wp e^{-2\beta t}\int_0^t dt_1\left(e^{(2\beta+i\delta)t_1}\hat{A}_1^\dagger(t_1)\hat{q}(t_1) + e^{(2\beta-i\delta)t_1}\hat{A}_1(t_1)\hat{q}^\dagger(t_1)\right) - \frac{2\omega_0}{\hbar}\wp e^{-2\beta t}\int_0^t dt_1\left(e^{(2\beta-i\delta)t_1}\hat{A}_2^\dagger(t_1)\hat{q}(t_1) + e^{(2\beta+i\delta)t_1}\hat{A}_2(t_1)\hat{q}^\dagger(t_1)\right). \quad (11)$$

In these equations, for convenience, we have substituted $\vec{\wp}\cdot\hat{\vec{A}}^+_{i,\,free}(0,t) \equiv \wp\hat{A}_i(t)$ and $\vec{\wp}\cdot\hat{\vec{A}}^-_{i,\,free}(0,t) \equiv \wp\hat{A}_i^\dagger(t)$. These coupled equations describe the time evolution of the atomic operators.

By making use of these equations the behavior of various observable quantities can be discussed. In fact, with the help of equations (10) and (11), the averages can be calculated once the initial states of the atom and field are specified. We assume that the driving fields are produced by two separate DPOs operating below threshold [20,21].

The intracavity fields of such an oscillator can be described by two real Gaussian processes in positive-P representation. Let a_i and $a_i^\dagger (i = 1, 2)$ denote the annihilation and creation operators, respectively, for the intracavity fields of two DPOs with their rapid time dependence removed. The statistical properties of the fields are completely specified by the steady-state correlation functions [9]:

$$\left\langle\hat{a}_i^\dagger(t_1)\hat{a}_j(t_2)\right\rangle = \frac{\kappa_i\epsilon_i}{4}\left[\frac{e^{-\lambda_1^{(i)}|t_1-t_2|}}{\lambda_1^{(i)}} - \frac{e^{-\lambda_2^{(i)}|t_1-t_2|}}{\lambda_2^{(i)}}\right]\delta_{ij}, \quad (12)$$

$$\langle\hat{a}_i(t_1)\hat{a}_j(t_2)\rangle = e^{i\phi_i}\frac{\kappa_i\epsilon_i}{4}\left[\frac{e^{-\lambda_1^{(i)}|t_1-t_2|}}{\lambda_1^{(i)}} + \frac{e^{-\lambda_2^{(i)}|t_1-t_2|}}{\lambda_2^{(i)}}\right]\delta_{ij} = \left\langle\hat{a}_i^\dagger(t_1)\hat{a}_j^\dagger(t_2)\right\rangle^*, \qquad (i = 1, 2); \quad (13)$$

in which κ_i is the non-linear coupling constant between the second harmonic pump field and the sub-harmonic field. $\epsilon_i (i = 1, 2)$ is normalized pump amplitude for the DPO, $\phi_i (i = 1, 2)$ is a phase angle ($\kappa_i\epsilon_i = |\kappa_i\epsilon_i|e^{i\phi_i}$), and the decay constants $\lambda_1^{(i)}$ and $\lambda_2^{(i)}$ can be expressed in terms of cavity linewidth γ_i and the pump amplitude ϵ_i by

$$\lambda_1^{(i)} = \gamma_i - |\kappa_i\epsilon|, \quad (14)$$

$$\lambda_2^{(i)} = \gamma_i + |\kappa_i\epsilon|, \qquad (i = 1, 2), \quad (15)$$

respectively. The correlation functions of the driving field $\hat{A}_{i,free}(0,t) \equiv \hat{A}_i(t)$ at the position $r = 0$ of the atom are given by

$$\left\langle\hat{A}_i^+(t_1)\hat{A}_i(t_2)\right\rangle = \mathcal{P}_i\left\langle\hat{a}_i^+(t_{1r})\hat{a}_i(t_{2r})\right\rangle, \quad (16)$$

$$\left\langle\hat{A}_i(t_1)\hat{A}_i(t_2)\right\rangle = \mathcal{P}_i\left\langle\hat{a}_i(t_{1r})\hat{a}_i(t_{2r})\right\rangle, \quad (17)$$

$$\hat{S}_z(t)+1/2 = e^{-2\beta t}\left[\hat{S}_z(0)+1/2\right] - \frac{\omega_0}{\hbar}\wp e^{-2\beta t}\int_0^t dt_1\left[e^{(\beta+i\delta)t_1}\hat{A}_1^\dagger(t_1)\hat{q}(0) + e^{(\beta-i\delta)t_1}\hat{A}_1(t_1)\hat{q}^\dagger(0)\right]$$
$$- \frac{\omega_0}{\hbar}\wp e^{-2\beta t}\int_0^t dt_1\left[e^{(\beta-i\delta)t_1}\hat{A}_2^\dagger(t_1)\hat{q}(0) + e^{(\beta+i\delta)t_1}\hat{A}_2(t_1)\hat{q}^\dagger(0)\right],$$
$$- \frac{2\wp^2}{\hbar^2}e^{-2\beta t}\int_0^t dt_1 e^{(\beta+i\delta)t_1}\int_0^{t_1} dt_2\left[{\omega_0}^2 e^{(\beta-i\delta)t_2}\hat{A}_1^\dagger(t_1)\hat{S}_z(t_2)\hat{A}_1(t_2) + {\omega_0}^2 e^{(\beta+i\delta)t_2}\hat{A}_1^\dagger(t_1)\hat{S}_z(t_2)\hat{A}_2(t_1)\right]$$
$$- \frac{2\wp^2}{\hbar^2}e^{-2\beta t}\int_0^t dt_1 e^{(\beta-i\delta)t_1}\int_0^{t_1} dt_2\left[{\omega_0}^2 e^{(\beta+i\delta)t_2}\hat{A}_1^\dagger(t_2)\hat{S}_z(t_2)\hat{A}_1(t_1) + \omega_0^2 e^{(\beta-i\delta)t_2}\hat{A}_2^\dagger(t_2)\hat{S}_z(t_2)\hat{A}_1(t_1)\right]$$
$$- \frac{2\wp^2}{\hbar^2}e^{-2\beta t}\int_0^t dt_1 e^{(\beta-i\delta)t_1}\int_0^{t_1} dt_2\left[\omega_0^2 e^{(\beta-i\delta)t_2}\hat{A}_2^\dagger(t_1)\hat{S}_z(t_2)\hat{A}_1(t_2) + {\omega_0}^2 e^{(\beta+i\delta)t_2}\hat{A}_2^\dagger(t_1)\hat{S}_z(t_2)\hat{A}_2(t_2)\right]$$
$$- \frac{2\wp^2}{\hbar^2}e^{-2\beta t}\int_0^t dt_1 e^{(\beta+i\delta)t_1}\int_0^{t_1} dt_2\left[\omega_0^2 e^{(\beta+i\delta)t_2}\hat{A}_1^\dagger(t_1)\hat{S}_z(t_2)\hat{A}_2(t_1) + {\omega_0}^2 e^{(\beta-i\delta)t_2}\hat{A}_2^\dagger(t_2)\hat{S}_z(t_2)\hat{A}_2(t_1)\right] \quad (20)$$

$$S_z^{(1)}(t) = \frac{\wp^2}{\hbar^2}e^{-2\beta t}\Bigg(\int_0^t dt_1 e^{(\beta+i\delta)t_1}\int_0^{t_1} dt_2\left[{\omega_0}^2 e^{(\beta-i\delta)t_2}\left\langle\hat{A}_1^\dagger(t_1)\hat{A}_1(t_2)\right\rangle + \omega_0^2 e^{(\beta+i\delta)t_2}\left\langle\hat{A}_1^\dagger(t_1)\hat{A}_2(t_2)\right\rangle\right]$$
$$+\int_0^t dt_1 e^{(\beta-i\delta)t_1}\int_0^{t_1} dt_2\left[{\omega_0}^2 e^{(\beta+i\delta)t_2}\left\langle\hat{A}_1^\dagger(t_2)\hat{A}_1(t_1)\right\rangle + \omega_0^2 e^{(\beta+i\delta)t_2}\left\langle\hat{A}_2^\dagger(t_2)\hat{A}_1(t_1)\right\rangle\right]$$
$$+\int_0^t dt_1 e^{(\beta-i\delta)t_1}\int_0^{t_1} dt_2\left[\omega_0^2 e^{(\beta-i\delta)t_2}\left\langle\hat{A}_2^\dagger(t_1)\hat{A}_1(t_2)\right\rangle + {\omega_0}^2 e^{(\beta+i\delta)t_2}\left\langle\hat{A}_2^\dagger(t_1)\hat{A}_2(t_2)\right\rangle\right]$$
$$+\int_0^t dt_1 e^{(\beta+i\delta)t_1}\int_0^{t_1} dt_2\left[\omega_0^2 e^{(\beta+i\delta)t_2}\left\langle\hat{A}_1^\dagger(t_2)\hat{A}_2(t_1)\right\rangle + {\omega_0}^2 e^{(\beta-i\delta)t_2}\left\langle\hat{A}_2^\dagger(t_2)\hat{A}_2(t_1)\right\rangle\right]\Bigg) \quad (22)$$

where $t_{1r}(t_{2r})$ denotes the time retarded for propagation from the DPO to the atom,

$$\mathcal{P}_i = 2\gamma_i\left[\frac{2\hbar}{\epsilon_0\omega_i c\rho}\right], \qquad i=1,2. \quad (18)$$

We assume that both the DPOs fields have the same cross-sectional area ($=\rho$), and the same bandwidth ($\gamma_1=\gamma_2=\gamma$). We also assume the same retarded propagation for the two DPOs. Then the set of equations (10) to (18) are simple enough to describe the response of the system driven by the bichromatic light produced by the DPOs.

3 The fluorescent intensity

The fluorescent photon flux density (number of photons per unit time) at position $\vec{r}$ in the radiation zone is given by [7]

$$\left\langle\hat{I}(r,t)\right\rangle = 2\beta\left[\frac{3\sin^2\psi}{8\pi r^2}\right]\left\langle\hat{S}_z(t-r/c)+1/2\right\rangle, \quad t\geq r/c, \quad (19)$$

where ψ is the angle between $\vec{r}$ and the dipole moment $\vec{\wp}$. Thus, the far field fluorescent intensity is directly related to the expectation value of the atomic inversion $\langle\hat{S}_z(t)+1/2\rangle$ and there is no contribution in (19) from the free field. We calculate atomic inversion by eliminating $\hat{q}(t)$ from equation (11) with the help of equation (10) and assuming the atom initially to be in the ground state. Then we obtain an integral equation for inversion as

see equation (20) above.

The solution of equation (20) for arbitrary field strength requires a knowledge of atom-field correlation of all orders and hence is quite difficult. However, one can use perturbation theory instead, in the weak-field limit, where the exciting field strength is such that the corresponding Rabi frequencies ($\Omega_\pm$) are small compared to the atom-dipole decay rate β. The Rabi frequencies $\Omega_\pm$ are defined in equation (24) in the following. The iteration of equation (20) for $\hat{S}_z+1/2$ can be done and after taking the expectation values, the results can be expressed as follows:

$$\left\langle\hat{S}_z(t)+1/2\right\rangle = S_z^{(1)}(t)+S_z^{(2)}(t)+... \quad (21)$$

The leading term on the right hand side of equation (21) is of the order of $(\Omega_\pm/\beta)^2$ and the second term is of the order of $(\Omega_\pm/\beta)^4$ and so on. For the leading term we have

see equation (22) above.

Equation (22) involves auto and cross-correlations of the field amplitudes. The autocorrelation functions are given by equations (12) and (13) and we assume that there are

$$\left\langle \hat{S}_z(t)+\frac{1}{2}\right\rangle = \frac{1}{4}\left(\frac{\Omega_+}{\beta}\right)^2 \left(e^{-\beta t}\frac{2\beta\left[\left(\beta+\lambda_1^{(1)}+\lambda_2^{(1)}\right)\left(\beta+\lambda_1^{(1)}\right)\left(\beta+\lambda_2^{(1)}\right)+\beta\delta^2\right]}{\left[\left(\beta+\lambda_1^{(1)}\right)^2+\delta^2)\right]\left[\left(\beta+\lambda_2^{(1)}\right)^2+\delta^2)\right]}\sinh(\beta t) \right.$$
$$-\frac{2\beta^2\lambda_2^{(1)}\left(\beta^2-\left(\lambda_1^{(1)}\right)^2+\delta^2\right)\left[\cos(\delta t)e^{-\left(\beta+\lambda_1^{(1)}\right)t}-e^{-2\beta t}\right]+4\delta^2\left(\lambda_1^{(1)}\right)^2\lambda_2^{(1)}\sin(\delta t)e^{-\left(\beta+\lambda_1^{(1)}\right)t}}{\left(\lambda_2^{(1)}-\lambda_1^{(1)}\right)\left(\beta^2-\left(\lambda_1^{(1)}\right)^2+\delta^2\right)^2+4\delta^2\left(\lambda_1^{(1)}\right)^2}$$
$$\left.+\frac{2\beta^2\lambda_1^{(1)}\left(\beta^2-\left(\lambda_2^{(1)}\right)^2+\delta^2\right)\left[\cos(\delta t)e^{-(\beta+\lambda_2^{(1)})t}-e^{-2\beta t}\right]+4\delta^2\left(\lambda_2^{(1)}\right)^2\lambda_1^{(1)}\sin(\delta t)e^{-\left(\beta+\lambda_1^{(1)}\right)t}}{\left(\lambda_2^{(1)}-\lambda_1^{(1)}\right)\left(\beta^2-\left(\lambda_2^{(1)}\right)^2+\delta^2\right)^2+4\delta^2\left(\lambda_2^{(1)}\right)^2}\right)$$
$$+\frac{1}{4}\left(\frac{\Omega_-}{\beta}\right)^2\left(\lambda_1^{(1)}\rightarrow\lambda_1^{(2)},\lambda_2^{(1)}\rightarrow\lambda_2^{(2)}\right) \qquad (23)$$

no cross-correlations between the fields of the two DPOs. Then using the autocorrelation functions only and carrying out the integration and proper simplification, we get, to the lowest order in $(\Omega_\pm/\beta)$,

see equation (23) above

where the Rabi frequencies $\Omega_\pm$ are given by

$$\Omega_\pm = \left(\frac{16\gamma\omega_0^2\wp}{\epsilon_0\hbar(\omega_0\pm\delta)c\rho}\right)^2\bar{n}, \qquad (24)$$

in which we have assumed the mean intracavity photon $(\bar{n})$ for the two DPOs to be equal. Since, the detuning $\delta \ll \omega_0$ so we can write $\Omega_+ \approx \Omega_-$ with negligible error.

Using equation (23) we can easily explain the growth of fluorescent light intensity as a function of time with the variation of parameters. As a check we note that for $\delta = 0$ we recover the results of reference [7]. In the case of monochromatic excitation ($\delta = 0$), the steady-state value of the fluorescent intensity is a sensitive function of the bandwidth of the squeezed field. For larger bandwidths (γ) of the squeezed fields there is a reduction in the steady-state fluorescent intensity because as the bandwidth increases the effective number of modes coupled to the atom reduces and so the effective field strength goes down [7]. Similar trends are obtained under bichromatic excitation also. However, it is interesting to see the behavior of fluorescent intensity with variation of δ/β.

In Figure 1 we plot the time evolution of the fluorescent intensity under bichromatic excitation with two squeezed fields for a typical set of parameters $\Omega_+/\beta = \Omega_-/\beta = 0.1$, and $\gamma/\beta = 1.0$. Curves A, B, C, D, and E are for $\delta/\beta = 0.5$, 1.0, 2.0, 3.0 and 5.0, respectively. For short times, in all cases, we see a tendency for ringing or oscillatory phenomenon which becomes more prominent as we increase the value of δ (see curves D and E). At the same time, we find that there is a drop in the steady-state value of the fluorescent intensity as we increase δ from zero (curve A) to a higher value (curve E). The oscillations in the fluorescent intensity are a result of mixing of two different

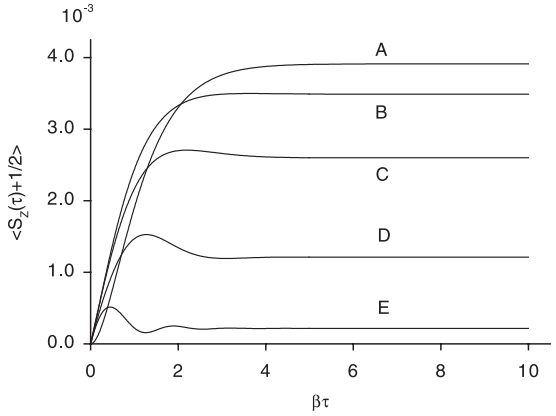

Fig. 1. Development of fluorescent light intensity proportional to $\langle S_z(\tau)+1/2\rangle$ as a function of scaled time $\beta\tau$ for several separations (i.e., δ/β) of the bichromatic fields with $\gamma/\beta = 1.0$ and $\Omega_+/\beta = \Omega_-/\beta = 0.1$. Curves A, B, C, D, and E are for $\delta/\beta = 0, 0.5, 1.0, 2.0$, and 5.0, respectively.

frequency fields (separated by frequency 2δ) when they simultaneously excite the same atom. They give rise to beating phenomenon in the emitted intensity. In other words, the atom excited under two weak fields at two slightly different frequencies emits fluorescence around these frequencies. These two components in fluorescence interfere, as there is coherence maintained between them because the emission is from the same atom. The frequency of fluorescent intensity oscillations increases as δ increases. At the same time, with increasing δ/β the two modes exciting the single atom get more and more detuned from the resonant transition frequency of the atom and less effective in exciting the atom leading to a smaller fluorescent intensity in the steady-state (τ very large). To further confirm this behavior we have plotted steady-state fluorescent intensity as a function of δ/β in Figure 2 keeping all other parameters the same as in Figure 1. Figure 2 clearly reveals how the steady-state fluorescent intensity drops down as δ/β increases.

$$\left\langle \hat{q}^\dagger(t)\left(\hat{S}_z(t+\tau)+\frac{1}{2}\right)\hat{q}(t)\right\rangle =$$
$$\frac{\omega_0^4}{\hbar^2}e^{-4\beta t-2\beta\tau}\int_0^t dt_1\int_t^{t+\tau}dt_2\int_t^{t_2}dt_3\int_0^t dt_4 e^{\beta(t_1+t_2+t_3+t_4)}e^{i\delta(t_1+t_2-t_3-t_4)}\left\langle A_1^\dagger(t_1)\hat{A}_1^\dagger(t_2)\hat{A}_1(t_3)\hat{A}_1(t_4)\right\rangle$$
$$+\frac{\omega_0^4}{\hbar^2}e^{-4\beta t-2\beta\tau}\int_0^t dt_1\int_t^{t+\tau}dt_2\int_t^{t_2}dt_3\int_0^t dt_4 e^{\beta(t_1+t_2+t_3+t_4)}e^{i\delta(-t_1-t_2+t_3+t_4)}\left\langle \hat{A}_2^\dagger(t_1)\hat{A}_2^\dagger(t_2)\hat{A}_2(t_3)\hat{A}_2(t_4)\right\rangle$$
$$+\frac{\omega_0^4}{\hbar^2}e^{-4\beta t-2\beta\tau}\int_0^t dt_1\int_t^{t+\tau}dt_2\int_t^{t_2}dt_3\int_0^t dt_4 e^{\beta(t_1+t_2+t_3+t_4)}e^{i\delta(t_1-t_2+t_3-t_4)}\left\langle \hat{A}_1^\dagger(t_1)\hat{A}_1^\dagger(t_3)\hat{A}_1(t_2)\hat{A}_1(t_4)\right\rangle$$
$$+\frac{\omega_0^4}{\hbar^2}e^{-4\beta t-2\beta\tau}\int_0^t dt_1\int_t^{t+\tau}dt_2\int_t^{t_2}dt_3\int_0^t dt_4 e^{\beta(t_1+t_2+t_3+t_4)}e^{i\delta(-t_1+t_2-t_3+t_4)}\left\langle \hat{A}_2^\dagger(t_1)\hat{A}_2^\dagger(t_3)\hat{A}_2(t_2)\hat{A}_2(t_4)\right\rangle \quad (29)$$

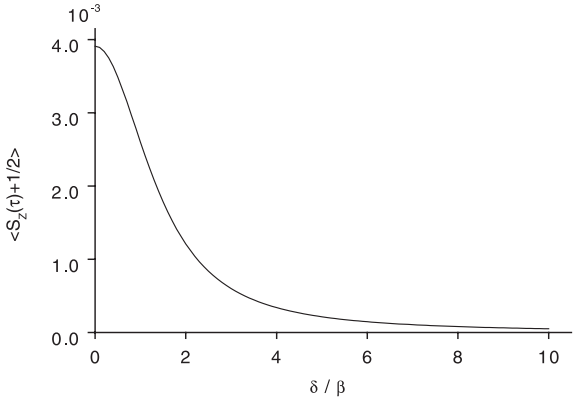

Fig. 2. The steady-state fluorescent light intensity proportional to $\langle S_z(\tau)+1/2\rangle$ as a function of δ/β with $\gamma/\beta = 1.0$, $\Omega_+/\beta = \Omega_-/\beta = 0.1$.

4 Two-time intensity correlation function

In order to investigate the statistical properties of the fluorescent field we make use of the second-order intensity-intensity correlation function defined by

$$g^{(2)}(\tau) \equiv \frac{\left\langle \mathcal{T} : \hat{I}(t)\hat{I}(t+\tau) : \right\rangle}{\left\langle \hat{I}(t)\right\rangle\left\langle \hat{I}(t+\tau)\right\rangle}. \quad (25)$$

This correlation function $g^{(2)}(\tau)$ represents the probability of detecting one photon at a time t followed by another at $t+\tau$. Here $\mathcal{T}$ means time ordering and :: denotes normal ordering of the operator products enclosed between the colons. It can be easily seen that $g^{(2)}(\tau)$ is independent of the detector's efficiency and is measurable in photon counting experiments. We can express the fluorescent light intensity $I(t)$ in terms of atomic operators with the help of equation (11). The normalized second-order intensity correlation function then reads

$$g^{(2)}(\tau) = \frac{\left\langle \hat{q}^\dagger(t_r)[\hat{S}_z(t_r+\tau)+1/2]\hat{q}(t_r)\right\rangle}{\langle \hat{q}^\dagger(t_r)\hat{q}(t_r)\rangle\,\langle \hat{q}^\dagger(t_r+\tau)\hat{q}(t_r+\tau)\rangle}, \quad (26)$$

where $t_r = (t - r/c)$. By making use of the operator properties, e.g., $[\hat{q}^\dagger(t)\hat{q}^\dagger(t)] = \hat{q}^\dagger[\hat{S}_z(t)+1/2] = [\hat{q}(t)\hat{q}(t)] = 0$, it can be shown that $g^{(2)}(\tau) \to 0$ at $\tau \to 0$ [7]. This implies that two photons cannot be simultaneously emitted by a two-level atom. Another important point is the factorization of $g^{(2)}(\tau)$ when a two-level atom is irradiated by coherent light. This is because photons in a coherent state are uncorrelated and a coherent state does not change via single-photon absorption process. In other words, after each emission of a photon the atom is de-excited to the ground state and the incident field is unchanged [7]. However, for a correlated state of light (e.g., a squeezed state) although the atom returns to the ground state after each emission the state of the field retains memory of the past because of the finite correlation time. We will come to this point again at the end of this section.

In order to evaluate $g^{(2)}(\tau)$ we rewrite the atomic operator given in equation (11) as

$$\hat{S}_z(t+\tau)+\frac{1}{2} = \left(\hat{S}_z+\frac{1}{2}\right)e^{-2\beta\tau} - \frac{\omega_0}{\hbar}\wp e^{-2\beta\tau}$$
$$\times\int_0^\tau dt_1 e^{2\beta\tau}\left[e^{i\delta(t+t_1)}\hat{A}_1^\dagger(t+t_1)\hat{q}(t+t_1)\right.$$
$$\left.+e^{-i\delta(t+t_1)}\hat{A}_1(t+t_1)\hat{q}^\dagger(t+t_1)\right]$$
$$-\frac{\omega_0}{\hbar}\wp e^{-2\beta\tau}\int_0^\tau dt_1 e^{2\beta\tau}$$
$$\times\left[e^{-i\delta(t+t_1)}\ \hat{A}_2^\dagger(t+t_1)\hat{q}(t+t_1)\right.$$
$$\left.+e^{i\delta(t+t_1)}\hat{A}_2(t+t_1)\hat{q}^\dagger(t+t_1)\right], \quad (27)$$

and the ladder operator as

$$\hat{q}(t+\tau) = \hat{q}(t)e^{-\beta\tau}$$
$$+\frac{2\wp\omega_0}{\hbar}e^{-\beta\tau}\int_0^\tau dt_1 e^{\beta t_1}e^{-i\delta(t+t_1)}\hat{A}_1(t+t_1)\hat{S}_z(t+t_1)$$
$$+\frac{2\wp\omega_0}{\hbar}e^{-\beta\tau}\int_0^\tau dt_1 e^{\beta t_1}e^{i\delta(t+t_1)}\hat{A}_2(t+t_1)\hat{S}_z(t+t_1). \quad (28)$$

Then, in the weak field limit the leading contribution to the numerator of $g^{(2)}(\tau)$ is given by

see equation (29) above.

$$\left\langle \hat{q}^{\dagger}(t)\left[\hat{S}_z(t+\tau)+\frac{1}{2}\right]\hat{q}(t)\right\rangle = \frac{1}{8}\left[\frac{\Omega_+}{\beta}\right]^4\left[\frac{\beta^2\lambda_1^{(1)}\lambda_2^{(1)}}{\lambda_2^{(1)}-\lambda_1^{(1)}}\right]^2\left\{\frac{\left(e^{-2\lambda_1^{(1)}\tau}-2\cos(\delta\tau)e^{-\left(\beta+\lambda_1^{(1)}\right)\tau}+e^{-2\beta\tau}\right)}{(\lambda_1^{(1)})^2\left[(\beta+\lambda_1^{(1)})^2+\delta^2\right]\left[\left(\beta-\lambda_1^{(1)}\right)^2+\delta^2\right]}\right.$$

$$+\frac{\left(e^{-2\lambda_2^{(1)}\tau}-2\cos(\delta\tau)e^{-\left(\beta+\lambda_2^{(1)}\right)\tau}+e^{-2\beta\tau}\right)}{\left(\lambda_2^{(1)}\right)^2\left[\left(\beta+\lambda_2^{(1)}\right)^2+\delta^2\right]\left[\left(\beta-\lambda_2^{(1)}\right)^2+\delta^2\right]}$$

$$+\left(\frac{\left(\lambda_1^{(1)}+\beta\right)^2\left(\lambda_1^{(1)}-\beta\right)^2+\delta^2\left(\beta+\lambda_1^{(1)}\right)}{2\lambda_1^{(1)}\beta^2\left[\left(\lambda_1^{(1)}+\beta\right)^2+\delta^2\right]\left[\left(\lambda_1^{(1)}-\beta\right)^2+\delta^2\right]}-\frac{\left(\lambda_2^{(1)}+\beta\right)^2(\lambda_2^{(1)}-\beta)^2+\delta^2\left(\beta+\lambda_2^{(1)}\right)}{2\lambda_2^{(1)}\beta^2\left[\left(\lambda_2^{(1)}+\beta\right)^2+\delta^2\right]\left[\left(\lambda_2^{(1)}-\beta\right)^2+\delta^2\right]}\right)$$

$$\times\left[\frac{\left(\beta-\lambda_1^{(1)}\right)\left(\left(\beta+\lambda_1^{(1)}\right)^2+\delta^2\right)e^{-2\beta\tau}}{\lambda_1^{(1)}\left[\left(\beta+\lambda_1^{(1)}\right)^2+\delta^2\right]\left[\left(\beta-\lambda_1^{(1)}\right)^2+\delta^2\right]}-\frac{2\beta\cos(\delta\tau)\left(\left(\beta+\lambda_1^{(1)}\right)\left(\beta-\lambda_1^{(1)}\right)+\delta^2\right)e^{-\left(\lambda_1^{(1)}+\beta\right)\tau}}{\lambda_1^{(1)}\left[\left(\beta+\lambda_1^{(1)}\right)^2+\delta^2\right]\left[\left(\beta-\lambda_1^{(1)}\right)^2+\delta^2\right]}\right.$$

$$+\frac{\left(\beta+\lambda_1^{(1)}\right)\left(\left(\beta-\lambda_1^{(1)}\right)^2+\delta^2\right)-4\delta\beta\lambda_1^{(1)}\sin(\delta\tau)e^{-\left(\beta+\lambda_1^{(1)}\right)\tau}}{\lambda_1^{(1)}\left[\left(\beta+\lambda_1^{(1)}\right)^2+\delta^2\right]\left[\left(\beta-\lambda_1^{(1)}\right)^2+\delta^2\right]}$$

$$-\frac{\left(\beta-\lambda_2^{(1)}\right)\left(\left(\beta+\lambda_2^{(1)}\right)^2+\delta^2\right)e^{-2\beta\tau}}{\lambda_2^{(1)}\left[\left(\beta+\lambda_2^{(1)}\right)^2+\delta^2\right]\left[\left(\beta-\lambda_2^{(1)}\right)^2+\delta^2\right]}+\frac{2\beta\cos(\delta\tau)\left(\left(\beta+\lambda_2^{(1)}\right)\left(\beta-\lambda_2^{(1)}\right)+\delta^2\right)e^{-\left(\lambda_2^{(1)}+\beta\right)\tau}}{\lambda_2^{(1)}\left[\left(\beta+\lambda_2^{(1)}\right)^2+\delta^2\right]\left[\left(\beta-\lambda_2^{(1)}\right)^2+\delta^2\right]}$$

$$\left.-\frac{\left(\beta+\lambda_2^{(1)}\right)\left(\left(\beta-\lambda_2^{(1)}\right)^2+\delta^2\right)-4\delta\beta\lambda_2^{(1)}\sin(\delta\tau)e^{-\left(\beta+\lambda_2^{(1)}\right)\tau}}{\lambda_2^{(1)}\left[\left(\beta+\lambda_2^{(1)}\right)^2+\delta^2\right]\left[\left(\beta-\lambda_2^{(1)}\right)^2+\delta^2\right]}\right]\Bigg\}+\frac{1}{8}\left[\frac{\Omega_-}{\beta}\right]^4\left[\frac{\beta^2\lambda_1^{(2)}\lambda_2^{(2)}}{\lambda_2^{(2)}-\lambda_1^{(2)}}\right]^2$$

$$\times\left[\text{terms same as above, but with } \lambda_1^{(1)}\to\lambda_1^{(2)},\ \lambda_2^{(1)}\to\lambda_2^{(2)}\right] \quad (31)$$

We can now express the fourth-order correlation functions appearing in equation (29) in terms of the second-order correlation functions because the driving field is Gaussian in time. Thus, for example [7],

$$\left\langle \hat{A}_i^{\dagger}(t_1)\hat{A}_i^{\dagger}(t_2)\hat{A}_i(t_3)\hat{A}_i(t_4)\right\rangle = \left\langle \hat{A}_i^{\dagger}(t_1)\hat{A}_i^{\dagger}(t_2)\rangle\langle\hat{A}_i(t_3)\hat{A}_i(t_4)\right\rangle + \left\langle \hat{A}_i^{\dagger}(t_1)\hat{A}_i(t_3)\right\rangle\left\langle \hat{A}_i^{\dagger}(t_2)\hat{A}_i(t_4)\right\rangle + \left\langle \hat{A}_i^{\dagger}(t_1)\hat{A}_i(t_4)\right\rangle\left\langle \hat{A}_i^{\dagger}(t_2)\hat{A}_i(t_3)\right\rangle, \quad (i=1,2). \quad (30)$$

After substituting equation (30) in equation (29) and carrying out some lengthy but straightforward integrations we obtain

see equation (31) above.

We can easily obtain an expression for $g^{(2)}(\tau)$ by substituting equation (31) into equation (26). We note that we recover the expression of $g^{(2)}(\tau)$ for monochromatic squeezed field excitation [7] under the condition $\delta/\beta = 0$.

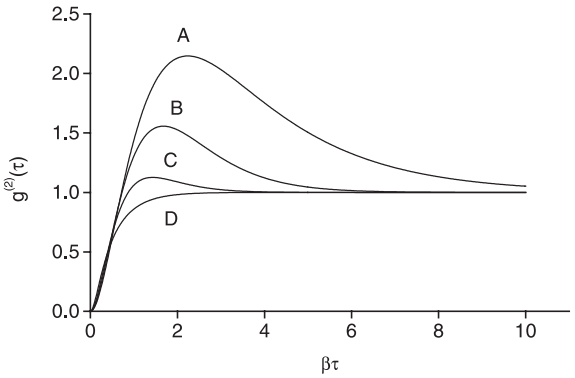

Fig. 3. The development of intensity-intensity correlation function $g^{(2)}(\tau)$ with respect to scaled time $\beta\tau$ for several different linewidths of the incident field under monochromatic excitation ($\delta/\beta = 0$). Curves A, B, C, and D, are for $\gamma/\beta = 0.5, 1.0, 2.0$, and 5.0, respectively.

To compare the results of bichromatic excitation with monochromatic excitation we plot, $g^{(2)}(\tau)$ as a function of τ in Figure 3 for various values of γ/β while keeping $\Omega_+/\beta = \Omega_-/\beta = 0.1$ fixed. The second-order

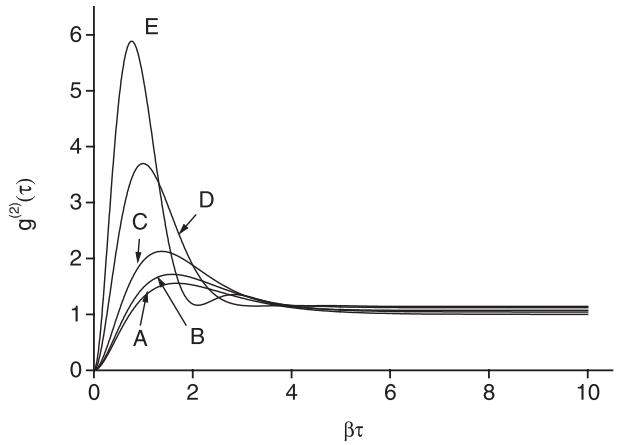

Fig. 4. The development of intensity-intensity correlation function $g^{(2)}(\tau)$ with respect to scaled time $\beta\tau$ for several separations (i.e., δ/β) of the bichromatic fields with $\gamma/\beta = 1.0$ and $\Omega_+/\beta = \Omega_-/\beta = 0.1$. Curves A, B, C, D, and E are for $\delta/\beta = 0, 0.5, 1.0, 2.0$, and 5.0, respectively.

intensity-intensity correlation function $g^{(2)}(\tau)$ starts from zero value for $\tau \to 0$ reflecting antibunching of photons. Also, this function approaches unity as $\tau \to \infty$. Here we observe delayed bunching of fluorescent photons because of intrinsic field-memory effect as the photons in squeezed light are pairwise correlated. This delayed antibunching is pronounced for $\beta \gg \lambda_1, \lambda_2$, and $\bar{n} \ll 1$ and is a reflection of pair-like photon sequence from the DPO. The atom is subjected to intense fields for brief periods. The second order intensity correlation is ideally suited for studying these two-photon events. With coherent light such effects are seen at much higher strengths. At longer times the function $g^2(\tau)$ factorizes as the DPO field correlations decay away. In Figure 4, we show $g^{(2)}(\tau)$ under bichromatic excitation for some selected parameter values from Figure 3, viz., $\Omega_+/\beta = \Omega_-/\beta = 0.1$ and $\gamma/\beta = 1$. We observe antibunching here also at the initial time ($g^{(2)}(\tau) = 0$ at $\tau = 0$) but as the time increases we find oscillatory behavior in $g^{(2)}(\tau)$. This oscillatory behavior becomes more prominent as the value of δ/β increases (curve E, Fig. 4). Also, there is an enhancement of delayed antibunching with increasing value of δ/β. This enhancement is on top of the one due to correlated nature of DPO photons. This enhancement arises due to the mixing of the two squeezed fields (separated in frequency by 2δ) which takes place in the atom when its is simultaneously interacting with two fields. Thus the emitted radiation from the atom interferes constructively or destructively at certain times depending on the value of δ relative to β and produces this effect in conformity with the oscillations in the fluorescent intensity discussed in Section 3. We have verified that the effect of delayed bunching diminishes with increasing γ. Also, at large time $g^{(2)}(\tau)$ reaches its steady-state value of 1 independent of the value of δ or β or γ. This reflects decay of field correlation at large times.

5 Summary

We have analyzed the problem involving interaction of a two-level atom with bichromatic squeezed fields under weak field excitation. The dynamics of the system is studied by solving the Heisenberg equations of motion. The results are valid for arbitrary bandwidths of the squeezed light. We have compared our results with those for monochromatic excitation under similar conditions. The main findings of this investigation include an oscillatory phenomenon in the transient fluorescent intensity and reduction of steady-state intensity with large separation of the frequencies of bichromatic fields. It is important to note that the oscillatory behavior is observed in a regime where monochromatic excitation does not exhibit any oscillatory behavior for the population inversion. This observed feature is an interference effect that arises due to a mixing of the field emitted by the atom at slightly different frequencies. The intensity-intensity correlation function also shows oscillations reminiscent of delayed bunching effect with coherent excitation in strong field limit. The enhancement of oscillatory behavior in $g^2(\tau)$ even in the weak field limit is reflection of both strong photon correlation of squeezed light and interference of the exciting fields. These effects, however, persists only for the short times. For long times, all field correlations eventually die down and we recover results which are independent of the nature of the fields and whether we have monochromatic or bichromatic excitation. This model may be useful in applications such as obtaining very low temperatures in laser cooling [22] experiments and laser outputs with sub-Poissonian statistics [23]. In fact, enhancement of Sisyphus cooling using a bichromatic standing wave has already been predicted [17]. If we use squeezed bichromatic fields in these calculations then it is possible to further enhance such cooling because of strong photon-pair correlations.

Funding supports from the National Science Foundation, ASTA, and the Office of Naval Research are acknowledged.

References

1. C.W. Gardiner, Phys. Rev. Lett. **56**, 1917 (1986)
2. H.J. Carmichael, A.S. Lane, D.F. Walls, Phys. Rev. Lett. **58**, 2539 (1987); H.J. Carmichael, S. Singh, R. Vyas, P.R. Rice, Phys. Rev. A **39**, 1200 (1989)
3. For example, see an excellent review by B.J. Dalton, Z. Ficek, S. Swain, J. Mod. Opt. **46**, 379 (1999) and references therein; also see special issues on squeezed states: J. Opt. Soc. Am. B **4**(10) (1987); J. Mod. Opt. **34**(6/7) (1987)
4. H. Ritsch, P. Zoller, Phys. Rev. A **38**, 4657 (1988)
5. A. Joshi, S.V. Lawande, Phys. Rev. A **41**, 2822 (1990); A. Joshi, R.R. Puri, Phys. Rev. A **43**, 6428 (1991); R.R. Puri, A. Joshi, R.K. Bullough, Int. J. Mod. Phys. B **5**, 3115 (1991); A. Joshi, R.R. Puri, Opt. Commun. **86**, 46 (1991); Phys. Rev. A **45**, 2025 (1992); Opt. Commun. **94**, 362 (1992); Int. J. Mod. Phys. B **8**, 121 (1994); A. Joshi, S.S. Hassan, J. Phys. B **30**, L557 (1997)

6. A. Messikh, R. Tanas, Z. Ficek, Phys. Rev. A **61**, 033811 (2000)
7. R. Vyas, S. Singh, Phys. Rev. A **45**, 8095 (1992)
8. I.E. Lyublinskaya, R. Vyas, Phys. Rev. A **48**, 3966 (1993)
9. R. Vyas, S. Singh, Opt. Lett. **14**, 1110 (1989); Phys. Rev. A **40**, 5147 (1989); A.B. Dodson, R. Vyas, Phys. Rev. A **47**, 3396 (1993)
10. J.P. Clemens, P.R. Rice, P.K. Rungta, R.J. Brecha, Phys. Rev. A **62**, 033802 (2000)
11. A.B. Matsko et al., Phys. Rev. A **66**, 043815 (2002)
12. R.S. Bennink, R.W. Boyd, Phys. Rev. A **66**, 053815 (2002)
13. P.T. Cochrane, T.C. Ralph, G.J. Milburn, Phys. Rev. A **65**, 062306 (2002)
14. S. Haroche, Ann. Phys. Fr. **6**, 189 (1971); G. Grynberg, P.R. Berman, Phys. Rev. A **39**, 4016 (1989); Y. Zhu, Q. Wu, A. Lezama, D.J. Gauthier, T.W. Mossberg, Phys. Rev. A **41**, R6574 (1990); S.P. Tewari, M.K. Kumari, Phys. Rev. A **41**, 5273 (1990); H.S. Freedhoff, Z. Chen, Phys. Rev. A **41**, 6013 (1990); G.S. Agarwal, Y. Zhu, D.J. Gauthier, T.W. Mossberg, J. Opt. Soc. Am. B **8**, 1163 (1990); W.M. Ruyten, J. Opt. Soc. Am. B **9**, 1892 (1992)
15. D.L. Aronstein, R.S. Bennink, R.W. Boyd, C.R. Stroud Jr, Phys. Rev. A **65**, 067401 (2002)
16. M. Jakob, G.Y. Kryuchkyan, Phys. Rev. A **61**, 053823 (2000)
17. R.G. Unanyan, S. Guerin, H.R. Jauslin, Phys. Rev. A **62**, 043407 (2000); S.K. Dutta, N.V. Morrow, G. Raithel, Phys. Rev. A **62**, 035401 (2000)
18. R.S. Bennik, R.W. Boyd, C.R. Strod Jr, V. Wong, Phys. Rev. A **63**, 033804 (2001)
19. H.J. Kimble, L. Mandel, Phys. Rev. A **13**, 2123 (1976); P.W. Milonni, Phys. Rev. **25** C, 1 (1976)
20. P.D. Drummond, K.J. McNeil, D.F. Walls, Opt. Acta **28**, 211 (1980); R. Graham, in *Quantum Statistics in Optics and Solid State Physics*, Springer Tracts in Modern Physics (Springer-Verlag, Berlin, 1973), Vol. 66
21. M.J. Collett, C.W. Gardiner, Phys. Rev. A **30**, 1386 (1984); M.J. Collett, D.F. Walls, Phys. Rev. A **32**, 2887 (1985)
22. J.I. Cirac, P. Zoller, Phys. Rev. A **47**, 2191 (1993)
23. H. Ritsch, M.A.M. Marte, D.F. Walls, Phys. Rev. A **38**, 3577 (1988)